Composite Structures xxx (2010) xxx–xxx

Contents lists available at ScienceDirect

Composite Structures

journal homepage: www.elsevier.com/locate/compstruct

Dynamic response and damage evolution in composite materials subjected to underwater explosive loading: An experimental and computational study

James LeBlanc [a,*], Arun Shukla [b]

[a] Naval Undersea Warfare Center (Division Newport), 1176 Howell Street, Newport, RI 02841, United States
[b] Department of Mechanical Engineering, University of Rhode Island, 203 Wales Hall, 92 Upper College Road, Kingston, RI 02881, United States

ARTICLE INFO

Article history:
Available online xxxx

Keywords:
Composite materials
Shock loading
Composite damage
Underwater explosion
Fluid–structure interaction

ABSTRACT

The effect of underwater shock loading on an E-Glass/Epoxy composite material has been studied. The work consists of experimental testing, utilizing a water filled conical shock tube and computational simulations, utilizing the commercially available LS-DYNA finite element code. Two test series have been performed and simulated: (1) a reduced energy series which allowed for the use of strain gages and (2) a series with increased energy which imparted material damage. The strain gage data and the computational results show a high level of correlation using the Russell error measure. The finite element models are also shown to be able to simulate the onset of material damage by both in-plane and delamination mechanisms.

Published by Elsevier Ltd.

1. Introduction

Within the naval community there is an interest in constructing new vehicles and structures from composite materials to exploit their high strength to weight ratios, resulting in lighter structural components. In a military environment these structures must be designed in a manner in which they will be able to survive an underwater explosion (UNDEX) event. This results in a need to understand the behavior of these materials not only at strain rates associated with static load levels (10^{-4}–10^{-3}) but also at loading rates many orders of magnitude higher (10^{-1}–10^{3}). The static response of composite materials is well understood while there is less of an understanding in terms of what happens to the same composite material when subjected to high loading rates. Currently the composite structures in use by the navy are designed with large safety factors to ensure that damage will not occur during a shock event. Due to these large safety factors the structures are often significantly over designed to the point that the full weight savings afforded by composite materials is not realized.

Historically there have been two experimental methodologies used to impart shock loading from a fluid to a structure: (1) explosives and (2) shock tubes. Although the use of explosives offers an ease of use, there are associated deficiencies such as spherical wave fronts and pressure signatures which are often spatially complex and difficult to measure. Shock tubes offer the advantage of plane wave fronts and wave parameters that are easily controlled and repeated.

When composite materials are subjected to loading conditions they may experience damage in the form of several distinct mechanisms occurring in the in-plane and through thickness directions. The in-plane mechanisms consist of fiber breakage and matrix cracking, while the through thickness damage is dominated by delamination of the plies.

Relevant experimental studies on composite materials have studied the material response over a range of loading rates. Work by Zaretsky et al. [1] and Yuan et al. [2] has studied the damage characteristics of composite materials when subjected to low velocity impacts while Mouritz [3] has studied the damage resulting from high rate UNDEX loading. LeBlanc et al. [4] have studied the effects of shock loading on three-dimensional woven composite materials. The results of these experimental studies however are limited to the study of post mortem properties of the materials. Once the loading, low or high rate, has been used to induce damage to the materials, the residual strength or fatigue properties are determined.

The study of damage mechanisms in composite materials can be grouped into three categories: (1) mathematical formulations, (2) numerical implementation into finite element software and (3) experimental studies. Matzenmiller et al. [5] have presented a mathematical model for damage of composite materials that develops a relationship between the level of material damage and the effective elastic properties of the material. For each of the significant damage mechanisms (fiber rupture, fiber buckling, matrix crushing, and matrix cracking) an internal variable describes the evolution of the damage as a function of loading. Based upon the expression representing each damage variable the effective elastic properties can be degraded when the variable reaches a

* Corresponding author. Tel.: +1 401 832 7920; fax: +1 401 832 7207.
E-mail address: JAMES.M.LEBLANC@Navy.mil (J. LeBlanc).

0263-8223/$ - see front matter Published by Elsevier Ltd.
doi:10.1016/j.compstruct.2010.02.017

Report Documentation Page

Form Approved
OMB No. 0704-0188

1. REPORT DATE	2. REPORT TYPE	3. DATES COVERED
2010		**00-00-2010 to 00-00-2010**

4. TITLE AND SUBTITLE	5a. CONTRACT NUMBER
Dynamic response and damage evolution in composite materials subjected to underwater explosive loading: An experimental and computational study	5b. GRANT NUMBER
	5c. PROGRAM ELEMENT NUMBER
6. AUTHOR(S)	5d. PROJECT NUMBER
	5e. TASK NUMBER
	5f. WORK UNIT NUMBER
7. PERFORMING ORGANIZATION NAME(S) AND ADDRESS(ES) **Naval Undersea Warfare Center,Division Newport,1176 Howell Street,Newport,RI,02841**	8. PERFORMING ORGANIZATION REPORT NUMBER
9. SPONSORING/MONITORING AGENCY NAME(S) AND ADDRESS(ES)	10. SPONSOR/MONITOR'S ACRONYM(S)
	11. SPONSOR/MONITOR'S REPORT NUMBER(S)

12. DISTRIBUTION/AVAILABILITY STATEMENT
Approved for public release; distribution unlimited

13. SUPPLEMENTARY NOTES

14. ABSTRACT
see report

15. SUBJECT TERMS

16. SECURITY CLASSIFICATION OF:			17. LIMITATION OF ABSTRACT	18. NUMBER OF PAGES	19a. NAME OF RESPONSIBLE PERSON
a. REPORT	b. ABSTRACT	c. THIS PAGE			
unclassified	**unclassified**	**unclassified**	**Same as Report (SAR)**	**10**	

critical value. As the mechanical properties must be continually updated to account for the damage degradation this methodology lends itself well to implementation into finite element codes.

The finite element modeling of damage in composites has been performed primarily on models simulating strain rates up to those representing drop test experiments with some work performed at the high strain rate regimes expected in shock loading. Material models are currently being implemented into existing commercial finite element codes (O'Daniel et al. [6], McGregor et al. [7], Williams and Vaziri [8]) however the validation work with these models has been limited to the low strain rate regime not experienced under blast/shock loading conditions. Recent publications involving computational modeling of damage progression in composites have utilized LS-DYNA and the Mat_162 (Mat_Composite_OPTION) material model which simulates fiber breakage, matrix cracking and delamination damage. This material model combines the progressive failure theory of Hashin and the damage mechanics approach of Matzenmiller et al. [5]. Gama et al. [9] and Xiao et al. [10] have published results from quasi-static punch shear loading experiments which correlate well with simulations utilizing the Mat_162 material model. Simulations of low velocity impact experiments have been documented in the work by Donadon et al. [11] and Hosseinzadeh et al. [12]. Furthermore Batra and Hassan [13] have studied the response of composites to UNDEX loading through numerical simulations; however there are no comparisons to experimental results. Although the dynamical experiments have been simulated, the results taken from these models have been limited to the prediction of damage area and final deformations rather than comparisons to transient response. Historically the material inputs are determined from quasi-static test data, an assumption which has been shown to be reasonable in simulations of composite materials subjected to high velocity impacts, Chan et al. [14]. This observation has been supported in the current work which investigates the underwater shock loading of composites.

Table 1
Cyply 1002 crossply – mechanical properties.

	N/m^2 ($lb/in.^2$)
Tensile modulus (0°)	23.4e9 (3.4e6)
Tensile modulus (90°)	23.4e9 (3.4e6)
Tensile strength (0°)	482e6 (70e3)
Tensile strength (90°)	482e6 (70e3)
Compressive strength (0°)	689e6 (100e3)
Compressive strength (90°)	689e6 (100e3)

2. Composite material

The composite material studied in this investigation is Cyply® 1002, a reinforced plastic manufactured by Cytec Engineered Materials. The material is a cured epoxy composite which utilizes a non-woven, parallel fiber construction. The fibers are continuous E-Glass filaments. The material is available in three unique constructions: (1) unidirectional, (2) cross-ply, and (3) isotropic. The cross-ply construction has been utilized in this study and has alternating plies of 0° and 90° with each ply having a thickness of 0.254 mm (0.01 in.). The cured material has an areal weight of 0.46 kg/m^2 (0.85 lb/yd^2) per ply (0.254 mm) and a specific gravity of 1.85. The resin content is 36 ± 3%. The material is available in thicknesses from 0.762 mm (0.03 in.) to 5.08 cm (2.0 in.). Thicknesses of 3.3 mm (0.130 in.) and 4.82 mm (0.190 in.) have been chosen for use in the current project with each thickness having 13 and 19 plies, respectively. Due to the odd number of plies there is an additional ply in the 0° direction. The laminate schedule for the 3.3 mm (0.130 in.) material is as follows [0/90/0/90/0/90/0/90/0/90/0/90/0] with a similar schedule for the 4.82 mm (0.190 in.) material, only with three more additional 0/90 layers. The material properties for the material are provided in Table 1.

3. Shock loading apparatus

A conical shock tube (CST) facility located at the Naval Undersea Warfare Center, Division Newport was utilized in the shock loading of the composite materials. The shock tube is a horizontally mounted, water filled tube with a conical internal shape, Fig. 1. The internal cone angle of the tube is 2.6° and simulates the free field pressure wave expansion in an open water environment. The tube is 5.25 m (207 in.) long from the charge location to the location of the test specimen and internally contains 98.4 L (26 gallons) of water at atmospheric pressure. The pressure shock wave is initiated by the detonation of an explosive charge at the breech end of the tube (left side of figure) which then proceeds down the length of the tube. Peak shock pressures from 9.65 MPa (1400 $lb/in.^2$) to 20.6 MPa (3000 $lb/in.^2$) can be obtained depending on the amount of explosive charge. A typical pressure profile obtained from the use of the tube is shown in Fig. 2. This figure illustrates the rapid pressure increase associated with the shock front followed by the exponential decay of the wave. This profile was obtained using the minimum amount of charge (M6 Blasting Cap – 1.32 g (0.00292 lb) TNT Equivalency) and is measured 50.8 cm (20 in.) from the impact face of the test specimen. The length of

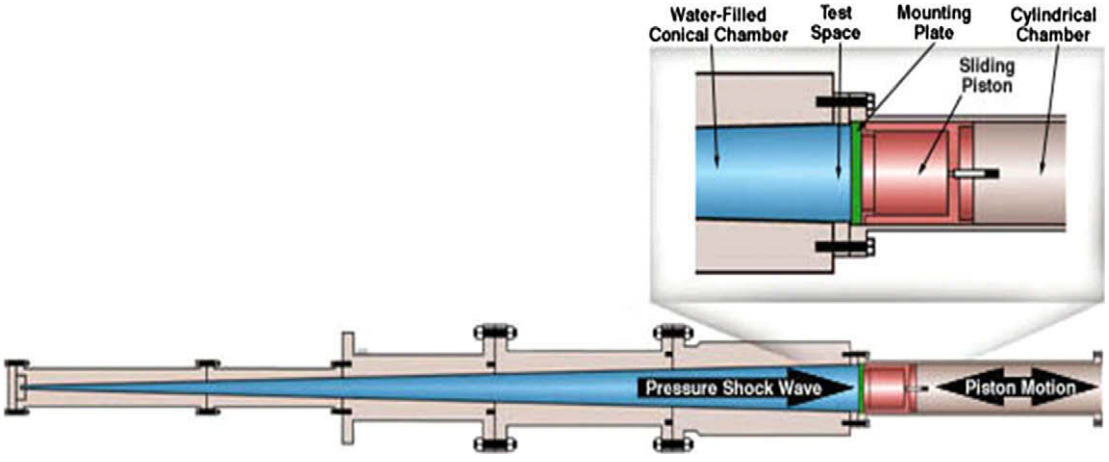

Fig. 1. Conical shock tube schematic.

Please cite this article in press as: LeBlanc J, Shukla A. Dynamic response and damage evolution in composite materials subjected to underwater explosive loading: An experimental and computational study. Compos Struct (2010), doi:10.1016/j.compstruct.2010.02.017

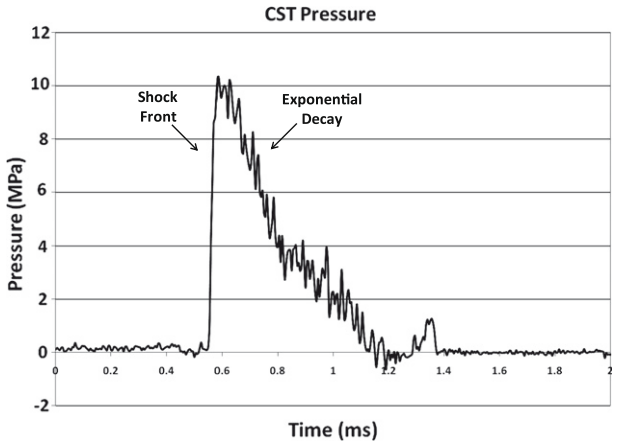

Fig. 2. Shock tube pressure profile.

the tube is sufficient so that plane wave conditions are nearly established at the test specimen.

The shock tube has the ability to be configured in two ways: (1) utilizing a sliding piston, and (2) the piston removed and replaced by a fixed end cap. The purpose of the sliding piston is to absorb energy in order to reduce the loading that the specimen will experience when the weight of the explosive charge cannot be reduced further. The fixed end cap configuration allows the test specimen to absorb the full energy of the pressure wave. Both configurations have been utilized in this study. The reasons will discuss later in the paper.

Mounting fixtures have been designed such that the test specimens are air backed with fully clamped edges. The specimens are 26.54 cm (10.45 in.) in overall diameter with a 22.8 cm (9 in.) unsupported middle section. The mounting arrangements for both tube configurations, slider included and fixed end cap, are shown in Fig. 3a and b respectively.

4. Experimental testing

Shock testing of the composite material has been performed with the CST in each of the two configurations, slider included and fixed end cap. The reason for utilizing the slider is that a lower loading level of the plates was desired than was possible utilizing the smallest amount of charge permissible (blasting cap only). Although this does not decrease the pressure loading that the plate experiences, the slider does absorb some of the energy that otherwise would be directed into the plate. Lower energy testing was used to decrease the loading level on the plates to the point where it would be possible to instrument the dry face of the test samples with strain gages with the expectation that they would remain attached during the shock event. The strain gage data served to provide a link for correlation between the experimental results and the finite element results to be discussed later. The use of the fixed end cap configuration allows the plate to absorb the full energy level and sustain a suitable level of damage for comparison to the finite element model results.

4.1. Testing with slider assembly

A series of two tests was performed utilizing the slider mechanism in order to capture strain gage data on the dry side of test samples. One test was performed with each of the two thickness materials, 3.3 mm (0.130 in.) and 4.82 mm (0.190 in.). The dry (non-impact) face of each of the samples was instrumented with four (4) tri-axial strain gages, which measured strains in the 0°, 45°, and 90° gage directions. The gages were mounted as seen in Fig. 4, with one gage located at the center of the panel and three gages located at a 7.62 cm (3 in.) radius from the center along the 0°, 45°, and 90° material directions. The choice of 7.62 cm (3 in.)" was based on having the gage at a reasonable distance from the center of the plate while not so close to the clamped edge that boundary effects became a factor. The strain gages were procured from Vishay Micro-Measurements with each having a gage length of 3.175 mm (0.125 in.) and a resistance of 350 Ω s (CEA-06-125UR-350). The gages are suitable for measurements up to 30,000 με. For both tests the strains were recorded at a sampling rate of 200 kHz.

For the test performed with the 4.82 mm (0.190 in.) thick test sample 9 of the 12 gages provided suitable output, while the other three suffered from de-bonding. The gages that provided output were the 0°, 45°, and 90° gage directions for the 3 gages located at the 7.62 cm (3 in.) radius from the center of the plate. The gage located at the center of the plate completely de-bonded from the test specimen. In the case of the test performed with the 3.3 mm (0.130 in.) plate only one suitable gage reading was obtained. This being the 0° gage direction on the gage located at a 7.62 cm (3 in.) radius along the 0° material direction. The low survival rate of the gages on the 3.3 mm (0.130 in.) plate can be expected as this plate has more out of plane flexure during the loading than the case of 4.82 mm (0.190 in.) plate. The strain profiles obtained from the test of the 4.82 mm (0.190 in.) plate for the three gages located along the 0° material direction are shown in Fig. 5. At this location the strain along the 0° direction is the largest in magnitude and the 90° is the smallest with the 45° strain falling in the middle. For the gages located along the 90° material direction a reversal of the magnitudes of the 0° and 90° strains is observed. This is expected as the radial strains associated with the principle flexure of the plate would be the largest. It is also observed that although the magnitudes of the strains are different for each gage direction, the time duration of each strain pulse is the same.

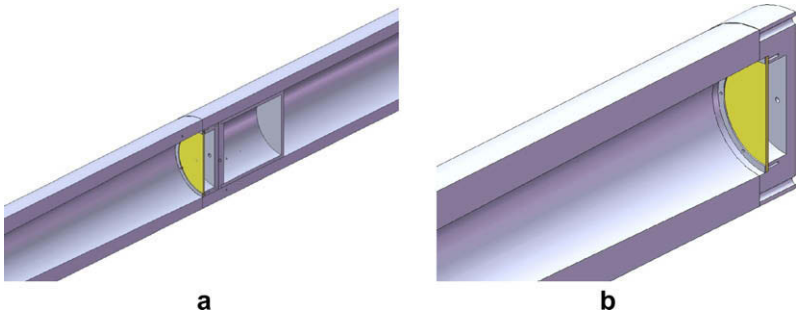

Fig. 3. (a) Slider mounting configuration, (b) fixed base mounting configuration.

Please cite this article in press as: LeBlanc J, Shukla A. Dynamic response and damage evolution in composite materials subjected to underwater explosive loading: An experimental and computational study. Compos Struct (2010), doi:10.1016/j.compstruct.2010.02.017

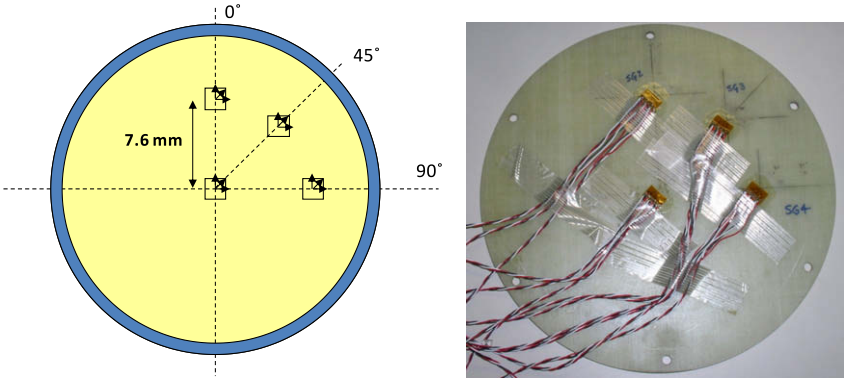

Fig. 4. Strain gage mounting pattern.

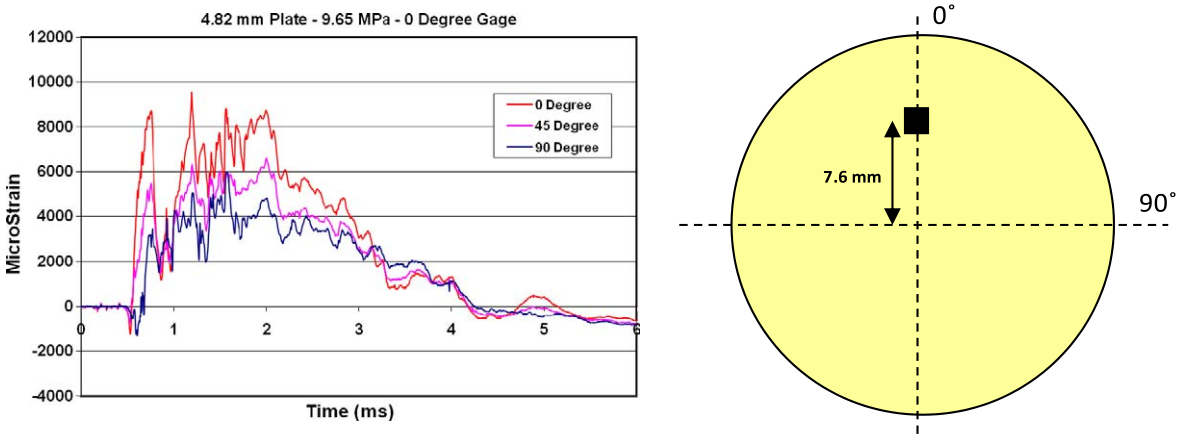

Fig. 5. Strain gage results, 4.82 mm (0.190 in.) plate at 9.65 MPa (1400 lb/in.^{2}) shock pressure.

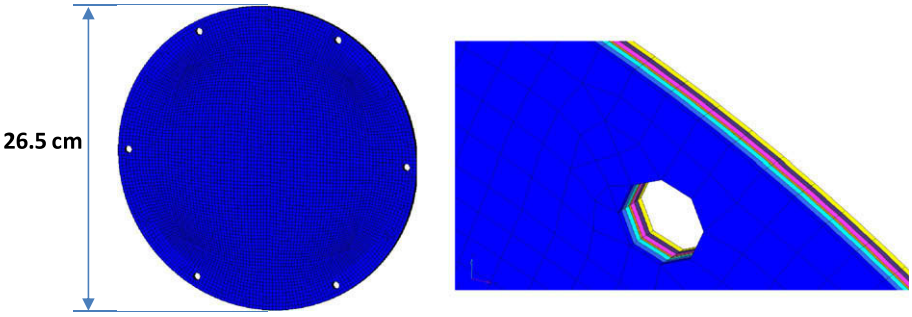

Fig. 6. Finite element model of composite plate.

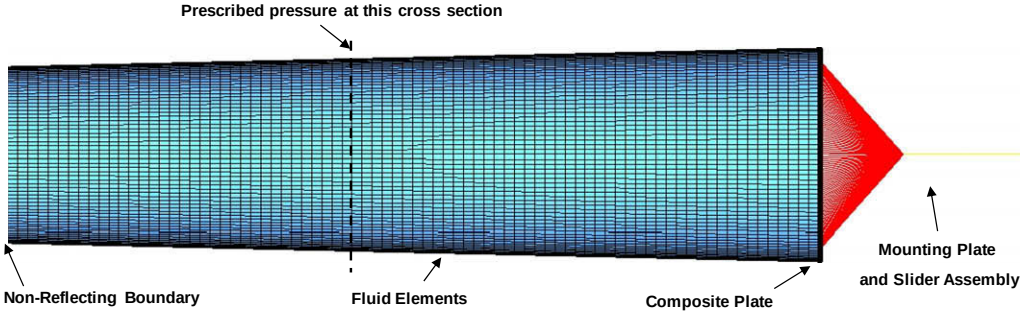

Fig. 7. CST finite element model.

Please cite this article in press as: LeBlanc J, Shukla A. Dynamic response and damage evolution in composite materials subjected to underwater explosive loading: An experimental and computational study. Compos Struct (2010), doi:10.1016/j.compstruct.2010.02.017

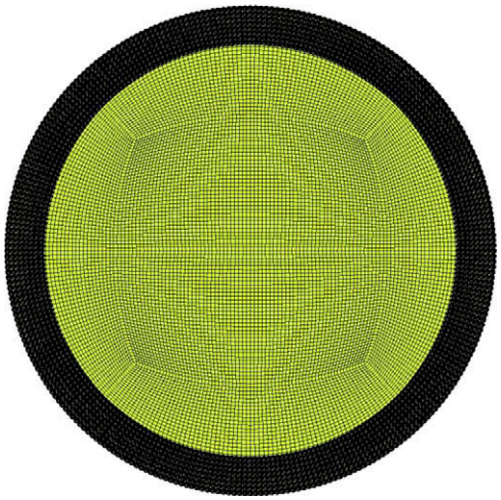

Fig. 8. Composite plate – clamped nodes.

5. Finite element modeling

Finite element modeling of the testing has been performed utilizing the LS-DYNA code available from the Livermore Software Technology Corporation (LSTC). All simulations are generated with Version 971, Release 3.1 and are run in double precision mode.

The composite plate in the simulations is modeled using solid brick elements with a constant stress element formulation (Type 1). The model of the 3.3 mm (0.130 in.) plate is shown in Fig. 6 and consists of seven layers of solid elements. Each layer represents a 0° and 90° combined ply (0.508 mm (0.02 in.) thick) with an additional single 0° layer (0.254 mm (0.01 in.) thick) in the middle of the layup. The holes represent the through bolt holes present in the test samples used for mounting the plate to the fixture. In the through thickness material direction the elements have an edge length of 0.508 mm (0.02 in.). The in-plane element edge lengths are approximately 2.54 mm (0.1 in.) with 95% of elements having an aspect ratio of 5:1 or less.

The LS-DYNA material model that is utilized in this work is Mat_Composite_Failure_*Option*_Model (Mat_059, Option = Solid). This is an orthotropic material definition capable of modeling the progressive failure of the material due to any of several failure criterion including tension/compression in the longitudinal and transverse directions, compression in the through thickness direction, and through thickness shear. Published descriptions of how each failure mode is handled are scarce, however there is some informal documentation available from LSTC. For each possible failure mode there is an internal variable which is checked throughout the analysis to determine if failure in that mode is present. Once failure due to one mode is triggered the load carrying ability of the material in that direction is reduced to zero. It is important to note that failure in one direction does not cause the element to be deleted. An element is only deleted from the analysis after it has failed in all directions and can no longer carry any load. The input material properties are those provided in Table 1. The material model inputs are derived from static tensile and compression testing with no modifications for strain rate effects. It was seen that the static properties provide reasonable results for shock loading conditions. This observation has been seen in literature addressing the ballistic impact problem as well. Chan et al. [14] have shown that the use of static properties is reasonable when applied to composite materials subjected to strain rates associated with high velocity impacts.

In the current modeling effort delamination damage is considered and is taken into account through the use of a surface-to-surface tiebreak contact definition. Using this approach each ply is modeled as a solid layer of elements but the nodes between plies are not equivalenced but rather tied together. The tie break definition initially ties the nodes between plies together to inhibit sliding motion. The nodal force at each node is monitored and checked against a predefined normal and shear force designated in the contact definition. If either the normal or shear force exceeds the defined value then the tie definition for that node is deleted and the node is free to slide. It is important to note that once the tie

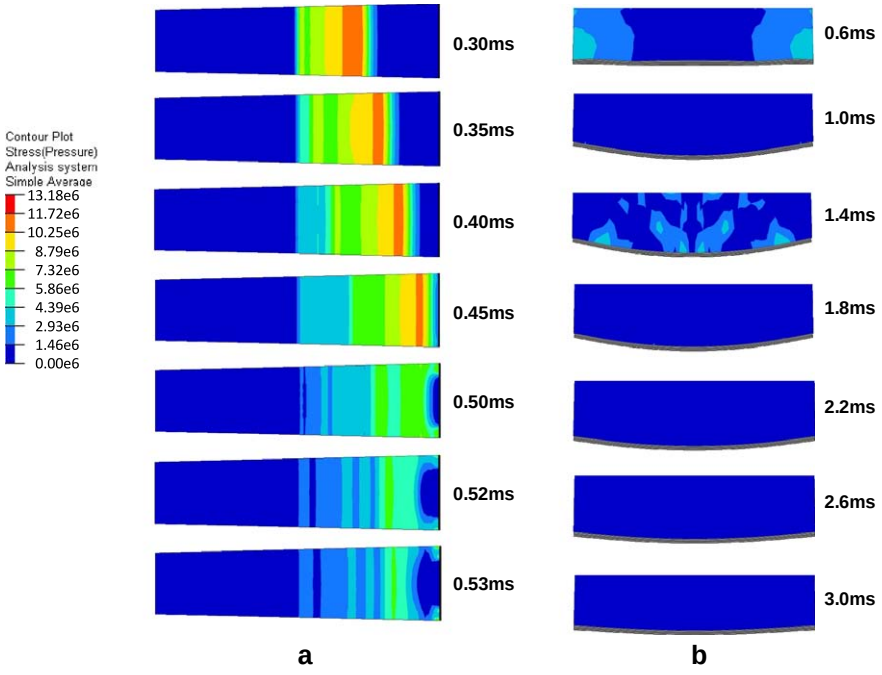

Fig. 9. (a) Fluid – plate interaction, (b) plate RESPONSE (units of Pa).

Please cite this article in press as: LeBlanc J, Shukla A. Dynamic response and damage evolution in composite materials subjected to underwater explosive loading: An experimental and computational study. Compos Struct (2010), doi:10.1016/j.compstruct.2010.02.017

component of the contact definition is deleted the contact for that node transitions to a standard definition. This allows the slave node to slide and separate from the master surface but not pass through it. Therefore, individual plies can separate but not pass thorough one another.

The complete finite element model of the CST test setup is shown in Fig. 7. The model consists of the internal fluid of the shock tube, the composite test sample, and the mounting plate/slider assembly. No numerical damping has been applied to the model. The fluid within the tube is considered in the simulation so as to capture the fluid–structure interaction (FSI) at the interface of the fluid and test plate. As will be shown later, this is a critical interaction to consider as the pressure loading on the plate is not uniform across its face. Only the first 1.01 m (40 in.) of the fluid extending from the test sample towards the charge location are modeled. This was deemed to be acceptable for two reasons: (1) the fluid is loaded with the pressure profile measured 50.8 cm (20 in.) from the test sample and (2) a non-reflecting boundary layer is applied at the charge side boundary of the fluid domain. The non-reflecting boundary allows the wave that is reflected from the plate to leave the fluid domain but not reenter. The fluid is modeled with solid elements and a null material definition. The use of the null material allows for the material to be defined with an equation of state (EOS) definition. A linear polynomial EOS is utilized for this model for which only the bulk modulus and density of the water is defined. This allows for an accurate propagation of the pressure wave in the water in a computationally efficient manner. The pressure load is applied as a plane wave at the location of the test pressure transducer. The pressure profile that was measured for each test is applied to the respective model. The fluid–structure interaction is handled through the use of a tied-surface-to-surface (LS-DYNA keyword *Contact_Tied_Surface_To_Surface) contact definition. In this method two contact surfaces (*Set_Segment) are defined for which the nodes are tied together. For the coupling of the fluid and composite plate the two surfaces are: (1) the fluid face where it contacts the plate, and (2) the plate face where it contacts the fluid. The mounting plate is simulated by a nodal constraint set that forces the nodes in the clamped area of the plate, Fig. 8, in the first and last ply to move together in the normal direction while they are free to move in-plane independently. The slider mechanism is accounted for through the use of a spring-damper beam definition. The stiffness and damping properties were determined by running a series of simulations in which the displacement of the mounting plate was compared to the response measured during the test with a linear variable displacement transducer (LVDT) which measured the displacement of the slider during the test.

6. Finite element simulation results

The finite element simulation of the shock tube testing allows for a visual full field representation of the interaction between the pressure wave and the composite plate, whereas the pressure profile obtained from the transducer gives only a single point history. The pressure field in the fluid as it interacts with and loads the plate, for the case of the 4.82 mm (0.190 in.) plate with the sli-

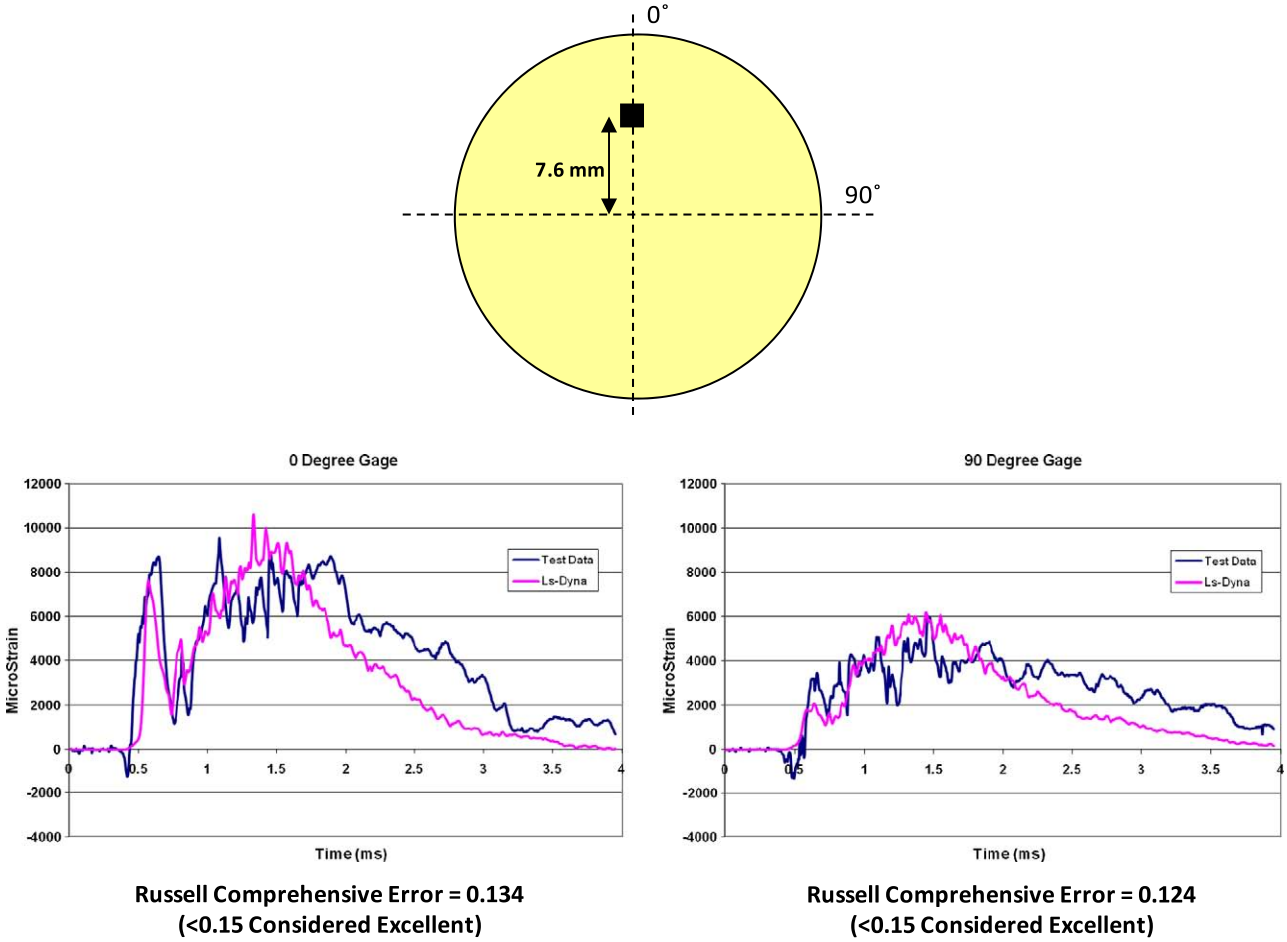

Fig. 10. Material 0° gage results.

Please cite this article in press as: LeBlanc J, Shukla A. Dynamic response and damage evolution in composite materials subjected to underwater explosive loading: An experimental and computational study. Compos Struct (2010), doi:10.1016/j.compstruct.2010.02.017

der mechanism, is shown in the left side of Fig. 9. The associated plate response is shown in right side of the figure. The time as shown in these figures, is the analysis time with zero taken at the initiation of the pressure field 50.8 cm (20 in.) from the test sample. Fig. 9 illustrates several key points. First, although the pressure wave is uniform (planar) prior to its impact with the test plate, the pressure becomes both complex and non-uniform when it interacts with and loads the plate itself. It is evident that there is a low pressure area that develops in the center of the plate while the clamped edge is loaded with high pressure. This can be attributed to the relatively low stiffness of the unsupported area of the plate as compared to the clamped edge of the plate where it is supported by the mounting ring. It is seen that the arrival and full reflection of the pressure wave take place over approximately 0.2 ms. The second point is that the loading of the plate and the associated response can be separated into two distinct time regimes. Where the pressure wave is fully reflected by 0.53 ms, the plate does not start to deform until 0.6 ms. The plate reaches full deformation at 1.8 ms and returns to its initial shape at 3 ms. Therefore there is clearly a time lag from when the plate is fully loaded due to the pressure wave, to when plate structurally responds. A similar result is seen for the case of the 3.3 mm (0.130 in.) plate test with the slider, as well as the testing done with the fixed end cap fixture.

6.1. Strain gage data – simulation correlation to test

The strain gage data that was captured during the experiments performed with the slider assembly is used as a basis to correlate and validate the finite element model results. The quality of the correlation between the test data and the numerical results in this study is quantified using the Russell Comprehensive Error measurement. The Russell error technique is one method which evaluates the differences in two transient data sets by quantifying the variation in magnitude and phase. The magnitude and phase error are then combined into a single error measure, the comprehensive error factor. The full derivation of the error measure is provided by Russell [15] with the phase, magnitude, and comprehensive error measures respectively given as:

$$RP = \frac{1}{\pi}\cos^{-1}\left(\frac{\sum c_i m_i}{\sqrt{\sum c_i^2 \sum m_i^2}}\right)$$

$$RM = \sin(m)\log_{10}(1+|m|)$$

$$RC = \sqrt{\frac{\pi}{4}(RM^2 + RP^2)}$$

In the above equations c_i and m_i represent the calculated (simulated) and measured responses respectively. Excellent, acceptable, and poor correlation using the Russell error measure is given as: Excellent – $RC \leqslant 0.15$, Acceptable – $0.15 < RC \leqslant 0.28$, and Poor $RC > 0.28$. The definition of these criteria levels are the result of a study that was undertaken to determine the correlation opinions of a team in support of a ship shock trial. A summary of the process used to determine the criteria is presented by Russell [16].

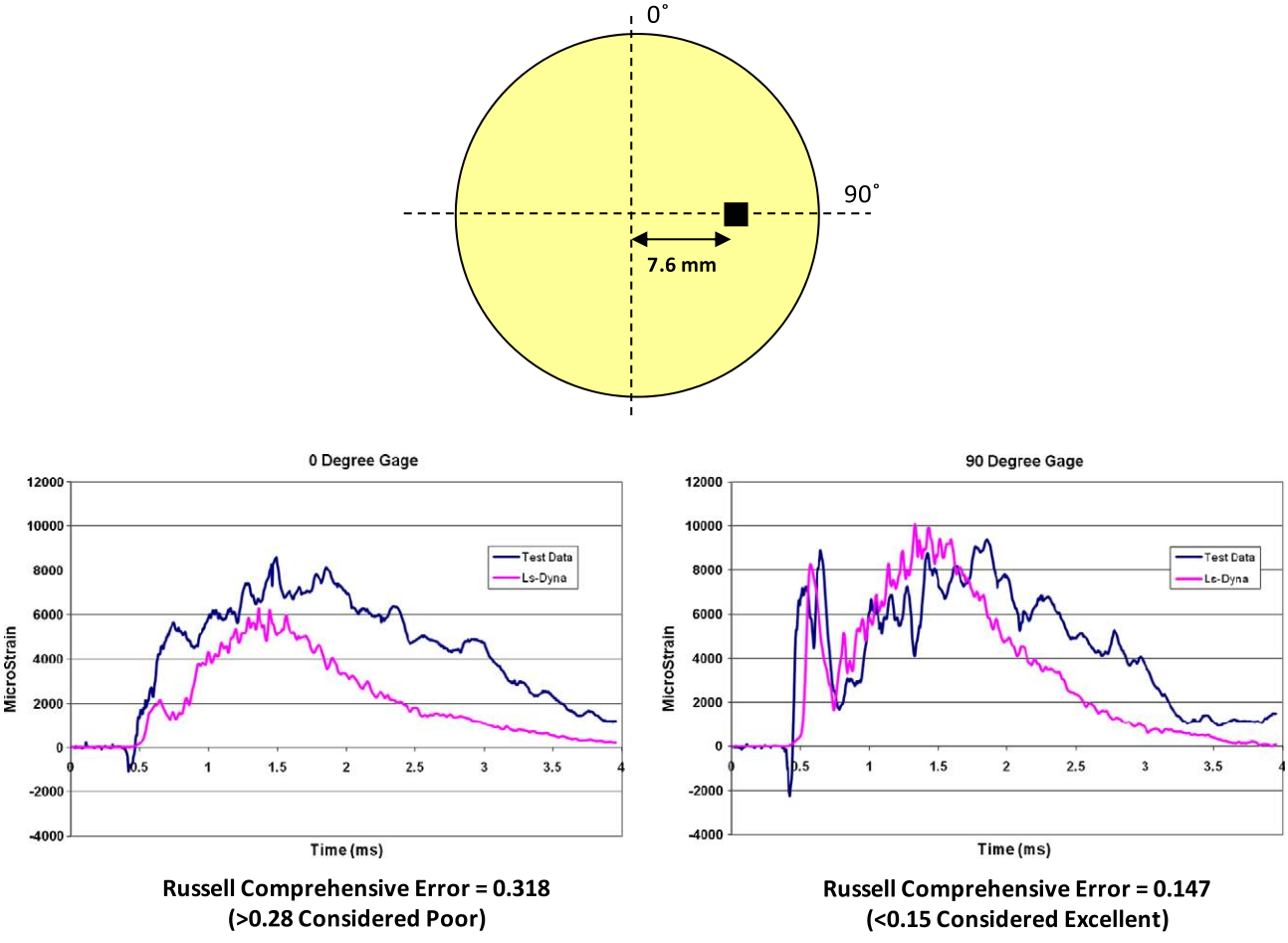

Fig. 11. Material 90° gage results.

Please cite this article in press as: LeBlanc J, Shukla A. Dynamic response and damage evolution in composite materials subjected to underwater explosive loading: An experimental and computational study. Compos Struct (2010), doi:10.1016/j.compstruct.2010.02.017

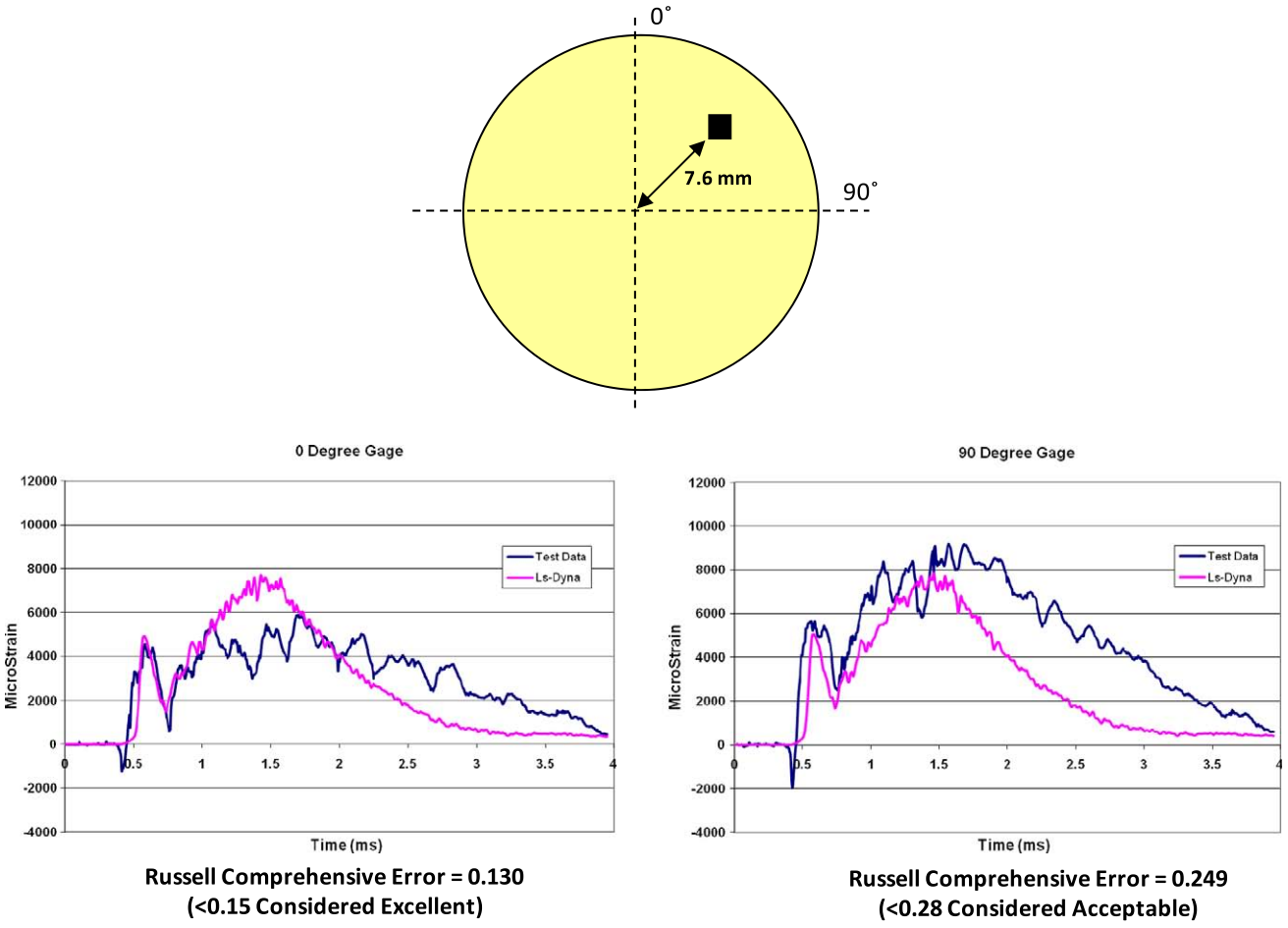

Fig. 12. Material 45° gage results.

The strain gage data comparisons for the shock test performed with the 4.82 mm (0.190 in.) thick plate and slider assembly is shown in Figs. 10–12 for the 0° and 90° gage directions. A summary of the Russell error for each of these tests as well as the gage that survived from the 3.3 mm (0.130 in.) test is provided in Table 2. From these graphical comparisons and error summary it is seen that there is a high level of correlation between the experimental results and the computational simulations. Five of the six strain profiles that are compared from the 4.82 mm (0.190 in.) plate thick test fall within the acceptable regime, including four in the excellent regime. The gage that remained attached from the 3.3 mm (0.130 in.) test also shows acceptable correlation. This level of agreement between the test and the finite element data is encouraging since strain gage data is notoriously difficult to correlate to and match with simulations.

Table 2
Russell error summary.

4.82 mm Plate – 9.65 MPa shock pressure	
Gage	Comprehensive
4	0.124
6	0.134
7	0.249
9	0.130
10	0.147
12	0.318
3.3 mm Plate – 9.65 MPa shock pressure	
6	0.187

<0.15 – Excellent.
<0.28 – Acceptable.
>0.28 – Poor.

7. Damage mechanisms – simulation correlation to test

The series of testing performed using the fixed end cap mounting fixture allowed for the full energy generated by the explosion to be absorbed by the test panel, as opposed to the slider mechanism which absorbed a portion of the energy. As a result of this increased load on the test plates in this configuration the panels sustained more severe surface and internal damage. The damage that was imparted to the sample during a typical test is shown in the left image of Fig. 13. This figure is from the 3.3 mm (0.130 in.) thick plate that was tested at a shock pressure of 11.7 MPa (1700 lb/in.^{2}). The corresponding finite element model result is shown in the right side image. The image of the test sample has been backlit to highlight the internal delamination that has occurred.

From these two images several qualitative observations can be made. First, both the experimental and computational results show that there are two cracks that initiate from the through holes located at the top and bottom (0° material direction) of the sample. These cracks propagate to a final length of approximately 6.35 cm (2.5 in.) in the experimental test sample and approximately 7.62 cm (3 in.) in the computational result. In both results the cracks run along the 0° material direction. The second observation

Please cite this article in press as: LeBlanc J, Shukla A. Dynamic response and damage evolution in composite materials subjected to underwater explosive loading: An experimental and computational study. Compos Struct (2010), doi:10.1016/j.compstruct.2010.02.017

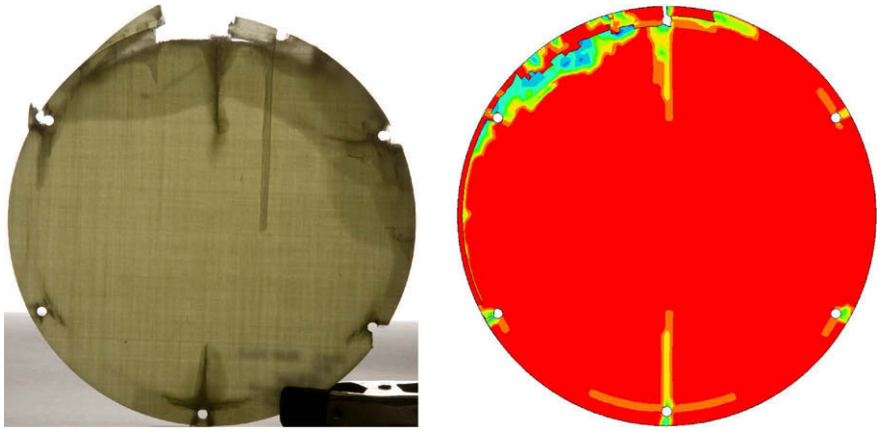

Fig. 13. (a) Material damage DURING test, (b) material damage FROM simulation.

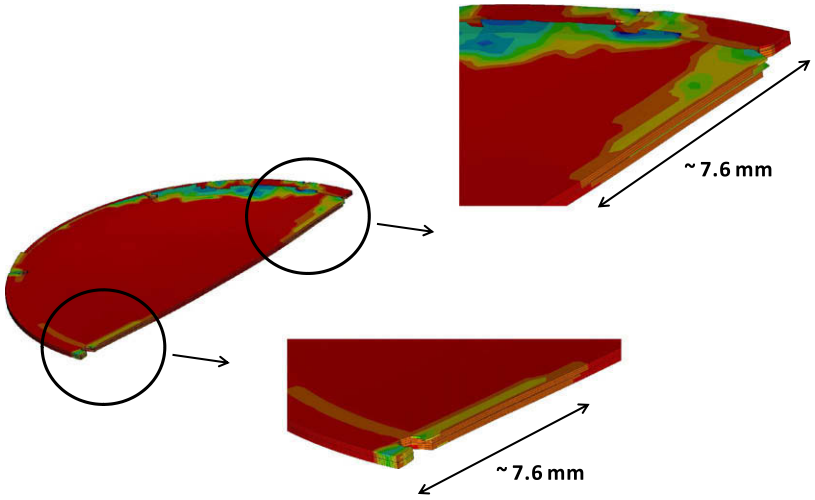

Fig. 14. Finite element model delamination.

is that there is material damage located between each of the holes and the edge of the sample, which was also predicted by the simulation. It is important to note that an initial finite element model of the plate was made in which the holes were omitted. This model developed neither the localized damage near the hole locations nor the crack along the 0° direction. This highlights two key aspects of this type of experimental and computational work. The first is that the damage that is observed is likely initiated due to the stress concentrations induced by the interaction of the mounting bolts and the plate as the material flexes and pulls towards the center of the plate during deformation. The second is that when undertaking small scale testing, where edge effects and geometric discontinuities can play a key part in the material response, it is important to include these features in the computational model. Otherwise the amount of damage predicted by the simulation will be less than that seen in the experimental component.

In the left image of Fig. 13 there is a region of delamination damage that developed along the top edge of the test specimen. This delamination zone extends from the edge of the plate inward to a radial distance of ~50.8 mm (2 in.) between the 10 and 3 O'clock positions. In the computational model this delamination zone also develops, Fig. 14, but it occurs both along the top and bottom edges. The delamination in the finite element model extends from the edge inward to a radial distance of 7.62 cm (3 in.). Although the amount of delamination is somewhat larger in the computational model than is observed in the test it is encouraging that the model is able to predict the onset of the delamination itself and propagate it to a comparable distance. In the current model the choice of a delamination criterion was taken to be 34.4 MPa (5000 lb/in.^{2}) for both tensile and shear stresses. The choice of this value was based on discussions of the developer of the material model (Materials Sciences Corporation). Based on these discussions it was determined that based on past experience an appropriate knock down factor for the delamination criteria is approximately one-half of the tensile strength of the pure epoxy. The degradation by ½ of the tensile strength accounts for voids and interfacial defects/flaws between the layers of fibers during the manufacturing of the material. The exact epoxy resin formula is held as proprietary by the material manufacturer however published values for the tensile strength of epoxy place the value between 27.5 and 82.7 MPa (4000–12,000 lb/in.^{2}). Therefore the choice of 34.4 MPa (5000 lb/in.^{2}) is reasonable. During the development of the models several values as high as 82.7 MPa (12,000 lb/in.^{2}) were utilized to determine the effect of this value. When a high value is chosen the delamination damage does not occur and all plies remain in tied contact. If a low value is taken then the plies completely delaminate early on in the simulation and the results do not agree with the experimental results. More work is planned into the most efficient way to model the delamination parameters but is outside of the scope of the current study.

Please cite this article in press as: LeBlanc J, Shukla A. Dynamic response and damage evolution in composite materials subjected to underwater explosive loading: An experimental and computational study. Compos Struct (2010), doi:10.1016/j.compstruct.2010.02.017

8. Conclusions

A conical shock tube has been used to study the response of an E-Glass/Epoxy composite material subjected to underwater shock loading. Two test series have been performed along with corresponding finite element model development. One test series was performed in which a slider mechanism was used with the shock tube to absorb a portion of the shock energy. This allowed the energy imparted to the test specimen to be reduced to the point where strain gages bonded to the back face of the specimen would remain attached during the event. The strain gage data recorded during the experiments was correlated to the computational models by utilizing the Russell error. The Russell error comparisons showed that 6 out of 7 of the gages that survived the testing had acceptable error measures with four of the gages exhibiting excellent correlation. A second series of testing was performed in which the slider was replaced with a fixed base mounting fixture which allowed for all of the shock energy to be imparted to the specimen. The samples tested with this mounting fixture showed significant damage areas including fiber/matrix breakage as well as internal delamination. The corresponding finite element simulations were able to simulate the appropriate forms and extents of the damage areas. This work has shown the ability of the LS-DYNA material model Mat_Composite_Failure_Option_Model to realistically model the behavior of a composite material under shock loading conditions. It was shown that the static elastic and strength material properties provide reasonable results for shock loading conditions. This work has served to show that computational tools can serve to support experimental test results and show promise for use as an alternative to testing to support structural designs utilizing composite materials.

Acknowledgements

The financial support of the Naval Undersea Warfare Center (Division Newport) In-house Laboratory Independent Research program (ILIR) directed by Dr. Anthony Ruffa is greatly acknowledged. Arun Shukla would like to acknowledge the support of Office of Naval Research under Grant No. N00014-04-1-0268 to the University of Rhode Island.

References

[1] Zaretsky E, deBotton G, Perl M. The response of a glass fibers reinforced epoxy composite to an impact loading. Int J Solids Struct 2004;41:569–84.
[2] Yuan F, Tsai L, Prakash V, Rajendran AM, Dandeka D. Spall strength of glass fiber reinforced polymer composites. Int J Solids Struct 2007;44:7731–47.
[3] Mouritz AP. The effect of underwater explosion shock loading on the fatigue behaviour of GRP laminates. Composites 1995;26 (1).
[4] LeBlanc J, Shukla A, Rousseau C, Bogdanovich A. Shock loading of three-dimensional woven composite materials. Compos Struct 2007;79:344–55.
[5] Matzenmiller A, Lubliner J, Taylor RL. A constitutive model for anisotropic damage in fiber-composites. Mech Mater 1995;20:125–52.
[6] O'Daniel JL, Koudela KL, Krauthammer T. Numerical simulation and validation of distributed impact events. Int J Impact Eng 2005;31:1013–38.
[7] McGregor CJ, Vaziri R, Poursartip A, Xiao X. Simulation of progressive damage development in braided composite tubes under axial compression. Composites: Part A 2007;38:2247–59.
[8] Williams KV, Vaziri R. Application of a damage mechanics model for predicting the impact response of composite materials. Comput Struct 2001;79:997–1011.
[9] Gama B, Xiao J, Haque M, Yen C, Gillespie J. Experimental and numerical investigations on damage and delamination in thick plain weave S-2 glass composites under quasi-static punch shear loading. Center for Composite Materials, University of Delaware; 2004.
[10] Xiao J, Gama B, Gillespie J. Progressive damage and delamination in plain weave S-2 glass/SC-15 composites under quasi-static punch-shear loading. Compos Struct 2007;78:182–96.
[11] Donadon MV, Iannucci L, Falzon BG, Hodgkinson JM, de Almeida SFM. A progressive failure model for composite laminates subjected to low velocity impact damage. Comput Struct 2008;86:1232–52.
[12] Hosseinzadeh R, Shokrieh MM, Lessard L. Damage behavior of fiber reinforced composite plates subjected to drop weight impacts. Compos Sci Technol 2006;66:61–8.
[13] Batra RC, Hassan NM. Response of fiber reinforced composites to underwater explosive loads. Composites: Part B 2007;38:448–68.
[14] Chan S, Fawaz Z, Behdinan K, Amid R. Ballistic limit prediction using a numerical model with progressive damage capability. Compos Struct 2007;77:466–74.
[15] Russell DM. Error measures for comparing transient data, part I: development of a comprehensive error measure, part II: error measures case study. In: Proceedings of the 68th shock and vibration symposium; 3–6 November 1997.
[16] Russell DM. DDG53 Shock trial simulation acceptance criteria. In: 69th shock and vibration symposium; 12–19 October 1998.

Please cite this article in press as: LeBlanc J, Shukla A. Dynamic response and damage evolution in composite materials subjected to underwater explosive loading: An experimental and computational study. Compos Struct (2010), doi:10.1016/j.compstruct.2010.02.017